WASHINGTON STATE DEPARTMENT OF
Natural Resources
Doug Sutherland - Commissioner of Public Lands
Division of Geology and Earth Resources
Ron Teissere - State Geologist

Field Data for a Trench on the Canyon River Fault, Southeast Olympic Mountains, Washington

by Timothy J. Walsh and Robert L. Logan

2007

Disclaimer

This report has not been edited or reviewed for conformity with Division of Geology and Earth Resources standards and nomenclature.

This product is provided 'as is' without warranty of any kind, either expressed or implied, including, but not limited to, the implied warranties of merchantability and fitness for a particular purpose. In no event shall the Washington State Department of Natural Resources and the authors of this product will not be liable to the user of this product for any activity involving the product with respect to the following: (a) lost profits, lost savings, or any other consequential damages; (b) injury to persons or property; (c) a particular purpose; or (c) use of the product or results obtained from use of the product.

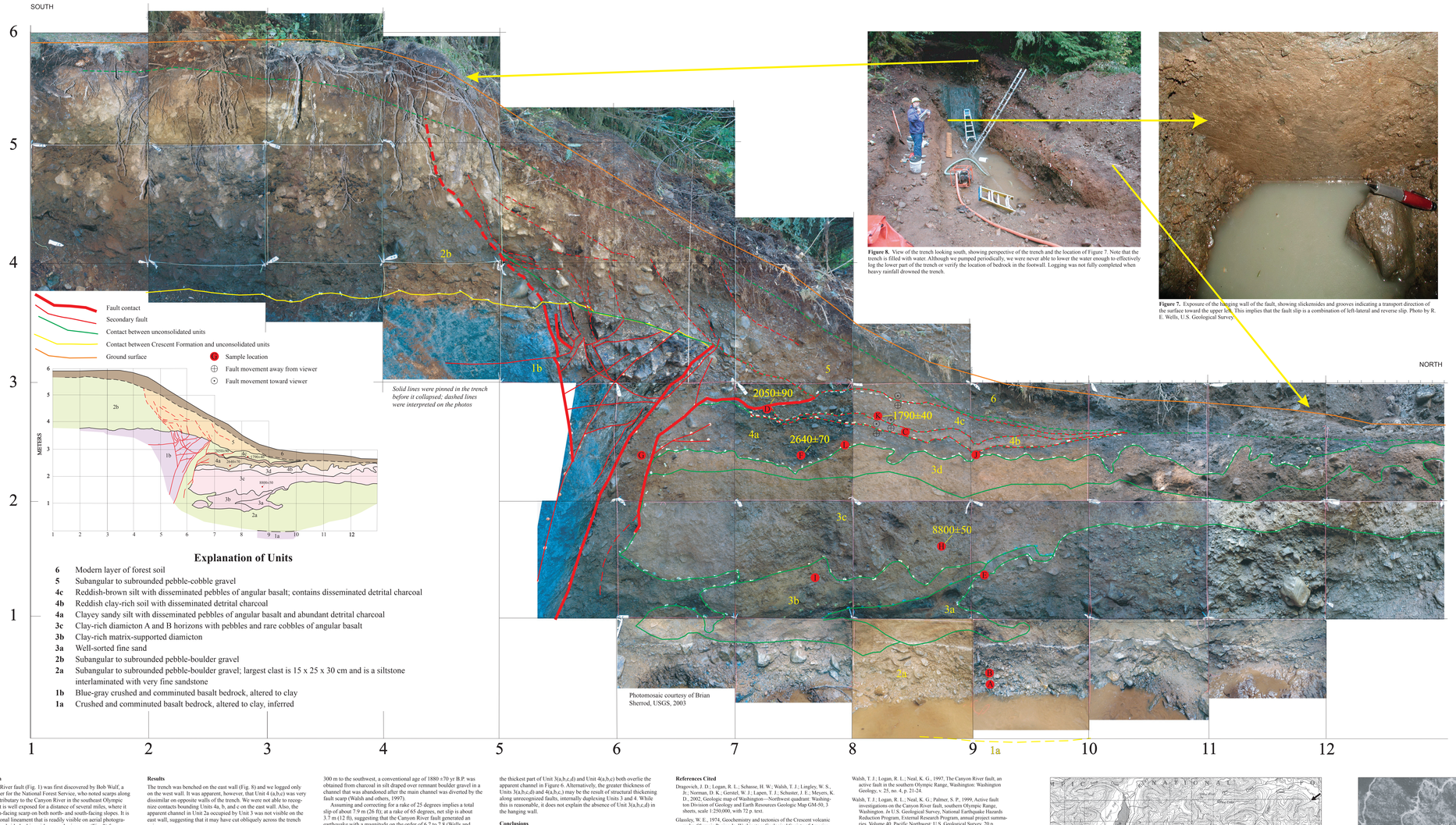

Explanation of Units

6 Modern layer of forest soil

5 Subangular to subrounded pebble-cobble gravel

4c Reddish-brown silt with disseminated pebbles of angular basalt; contains disseminated detrital charcoal

4b Reddish clay-rich soil with disseminated detrital charcoal

4a Clayey sandy silt with disseminated pebbles of angular basalt and abundant detrital charcoal

3c Clay-rich diamicton A and B horizons with pebbles and rare cobbles of angular basalt

3b Clay-rich matrix-supported diamicton

3a Well-sorted fine sand

2b Subangular to subrounded pebble-boulder gravel

2a Subangular to subrounded pebble-boulder gravel; largest clast is 15 x 25 x 30 cm and is a siltstone interlaminated with very fine sandstone

1b Blue-gray crushed and comminuted basalt bedrock, altered to clay

1a Crushed and comminuted basalt bedrock, altered to clay, inferred

Figure 8. View of the trench looking south, showing perspective of the trench and the location of Figure 7. Note that the trench is filled with water. Although we pumped periodically, we were never able to lower the water enough to effectively log the lower part of the trench or verify the location of bedrock in the footwall. Logging was not fully completed when heavy rainfall drowned the trench.

Figure 7. Exposure of the hanging wall of the fault, showing slickensides and grooves indicating a transport direction of the surface toward the upper left. This implies that the fault slip is a combination of left-lateral and reverse slip. Photo by R. E. Wells, U.S. Geological Survey.

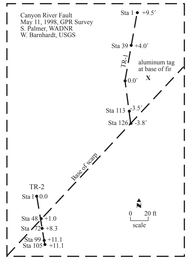

Figure 5. Location map for ground penetrating radar surveys (Walsh and others, 1999). TR-1 is the location of the trench.

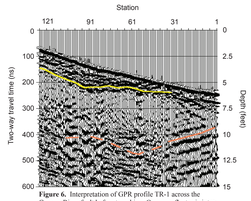

Figure 6. Interpretation of GPR profile TR-1 across the Canyon River fault before trenching. Orange reflector is interpreted as bedrock on the down-thrown side of the fault. Depth to bedrock at the base of the scarp is estimated to be approximately 3 to 4 m (10 to 13.5 ft). Yellow reflector is interpreted as a fan resulting from debris flows originating on the steep slope bounding the north side of the sag pond (Walsh and others, 1999).

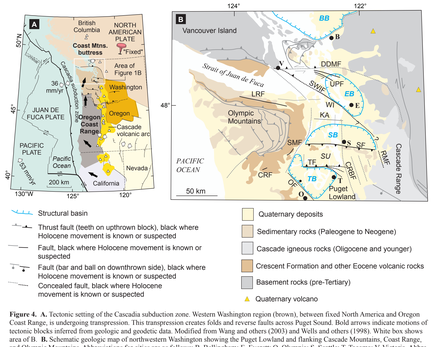

Figure 4. A. Tectonic setting of the Cascadia subduction zone. Western Washington region (brown), between fixed North America and Oregon Coast Range, is undergoing transpression. This transpression creates folds and reverse faults across Puget Sound. Bold arrows indicate motions of tectonic blocks inferred from geologic and geodetic data. Modified from Wang and others (2003) and Wells and others (1998). White box shows area of **B**. **B.** Schematic geologic map of northwestern Washington showing the Puget Lowland and flanking Cascade Mountains, Coast Range, and Olympic Mountains. Abbreviations for cities are as follows: B, Bellingham; E, Everett; O, Olympia; S, Seattle; T, Tacoma; V, Victoria. Abbreviations for faults (heavy lines) and other geologic features are as follows: BB, Bellingham basin; CRBF, Coast Range Border fault; CRF, Canyon River fault; DDMF, Darrington–Devils Mountain fault; EB, Everett basin; KA, Kingston arch; LRF, Little River fault; OF, Olympia fault; RMF, Rattlesnake Mountain fault; SB, Seattle basin; SF, Seattle fault; SMF, Saddle Mountain faults; SU, Seattle uplift; SWIF, Southern Whidbey Island fault; TB, Tacoma basin; TF, Tacoma fault; UPF, Utsalady Point and Strawberry Point faults. Geology from Walsh and others (1987), Dragovich and others (2002), and Johnson and others (2004). Modified from Sherrod and others (2004).

Introduction

The Canyon River fault (Fig. 1) was first discovered by Bob Wulf, a forest engineer for the National Forest Service, who noted scarps along an unnamed tributary to the Canyon River in the southeast Olympic Mountains. It is well exposed for a distance of several miles, where it forms a north-facing scarp on both north- and south-facing slopes. It is part of a regional lineament that is readily visible on aerial photography (Fig. 2) and side-looking airborne radar imagery (Fig. 3) for a distance of at least 40 mi. Separation is south over north, placing basalts of the upper Crescent Formation against the lower Crescent, as mapped by Tabor and Cady (1978). Faulting along this contact has been recognized in other parts of the Olympics (Glassley, 1974; Wilson and others, 1979). Lidar lineaments are also recognized at this approximate stratigraphic horizon within the Crescent both southwest and northeast of Lake Cushman and near Port Angeles (Haugerud and others, 2003) (Fig. 4). Walsh and others (1997) demonstrated that the fault was active in Holocene time and proposed several trench locations (Fig. 3). Walter Barnhardt and Stephen Palmer ran two ground penetrating radar (GPR) surveys at proposed trench site 3, demonstrating that bedrock in the footwall was reachable by trench (Figs. 5 and 6).

On September 13, 2003, we opened a trench at site TR-1 (locality 3 in Fig. 3. GPR survey TR-1 in Fig. 5). Even though it had been an unusually dry summer, the sag pond did not dry out completely. Water continually poured into the lower 2 ft of the trench, causing abundant sloughing that hindered logging of the lower part of the footwall and prevented us from exposing the bedrock surface, although the backhoe bucket scraped on it. Heavy rain three weeks later caused uncontrollable flooding and sloughing, forcing us to abandon the trench before we had finished logging and sampling. Nonetheless, we obtained much information from the trench.

Results

The trench was benched on the east wall (Fig. 8) and we logged only on the west wall. It was apparent, however, that Unit 4a(b,c) was very dissimilar on opposite walls of the trench. We were not able to recognize contacts bounding Units 4a, b, and c on the east wall. Also, the apparent channel in Unit 2a occupied by Unit 3 was not visible on the east wall, suggesting that it may have cut obliquely across the trench axis.

On the trench log, the orange line shows the modern ground surface. Red lines are faults and contacts are in green. The yellow contact marks the top of the bedrock surface. The obvious fault separation is high-angle reverse, striking N70E and dipping 70 degrees south. The abundant slickensides and grooves (some with the intact pebbles that carved the grooves still in place) on the highwall (Fig. 7) show a left-lateral sense of slip. The rake of one set of these grooves is 25 degrees, and a second set is 65 degrees. It was not clear that one set consistently truncated the other.

The net vertical separation of about 3.35 m, measured both on the top of the Crescent Formation and on the modern ground surface, and the presence of only one colluvial wedge (Unit 5) suggests a single event. The contacts between Units 4a, b, and c appear to be fault contacts near the fault scarp but they grade into a single unit away from the scarp. Their aggregate thickness near the scarp is about 1 m, but at a horizontal distance of 3 m from the scarp they thin to about 35 cm. Also, because there is no colluvium deposited between them but there is a thick colluvial wedge above them, we interpret slip along those contacts to be thrusting (drag) out of the plane of the trench wall (from west to east) synchronous with the slip on the primary fault plane. Radiocarbon ages on detrital charcoal in Units 4 a, b, and c do not overlap but they are limiting ages rather than event ages.

Conventional radiocarbon ages of detrital charcoal underlying the colluvial wedge are 2620 ±70, 2050 ±90, and 1790 ±40 yr B.P. About 300 m to the southwest, a conventional age of 1880 ±70 yr B.P. was obtained from charcoal in silt draped over remnant boulder gravel in a channel that was abandoned after the main channel was diverted by the fault scarp (Walsh and others, 1997).

Assuming and correcting for a rake of 25 degrees implies a total slip of about 7.9 m (26 ft); at a rake of 65 degrees, net slip is about 3.7 m (12 ft), suggesting that the Canyon River fault generated an earthquake with a magnitude on the order of 6.7 to 7.8 (Wells and Coppersmith, 1994) shortly after about 1880 yr B.P. The splaying from the main fault, much of which is thrust or high-angle reverse faulting, strongly suggests a positive flower structure, which further supports a significant strike-slip component.

Unit 3 (a,b,c,d) is about 1½ m thick in the footwall within about 2½ m of the fault, thinning to less than 1 m at a distance of 4 m from the fault. The net thickness of Unit 2a plus Unit 3(a,b,c,d) is approximately constant at 2½ m. Unit 3(a,b,c,d) is absent in the hanging wall and Unit 2b is about 2½ m thick at a distance of 4 m from the scarp. An angular cobble gravel that we infer to be the same as Unit 2a is a sliver faulted against bedrock on the hanging wall and against Unit 3 in the footwall.

Figure 8 shows the trench, looking southward and puts the trench in perspective.

Discussion

The difference between the stratigraphy of the hanging wall and footwall parts of the trench differs significantly. Unit 2a, which we interpret to be a noncohesive debris flow deposit or colluvium, is very similar to Unit 2b but is much thinner, at least adjacent to the fault. We interpret Unit 3(a,b,c,d), which appears to be channelized into 2b, to be a cohesive debris flow deposit. Because we do not recognize the channel on the east wall of the trench, we infer that it may have cut obliquely across the trench axis from southeast to northwest. However, the thickest part of Unit 3(a,b,c,d) and Unit 4(a,b,c) both overlie the apparent channel in Figure 6. Alternatively, the greater thickness of Units 3(a,b,c,d) and 4(a,b,c,) may be the result of structural thickening along unrecognized faults, internally duplexing Units 3 and 4. While this is reasonable, it does not explain the absence of Unit 3(a,b,c,d) in the hanging wall.

Conclusions

The Canyon River fault lies on a discontinuous lineament from south of Lake Wynoochee to near Lake Cushman, marked by a 3-m-high north-facing scarp. Motion on the fault was oblique reverse-left-lateral and was probably dominantly strike-slip. A single late Holocene event had a probable magnitude between about 7 to 7.5. The Wynoochee Dam was built in 1972 and the two Cushman dams were completed in 1926 and 1930 and were likely not designed to withstand an earthquake of that magnitude.

Acknowledgments

Brian Sherrod (USGS) was instrumental in making this investigation. He obtained permission for trenching from the U.S. Forest Service, supported the digging of the trench and the radiocarbon dating, and made the photomosaic on which we mapped. Steve Palmer (Geodesign, Inc.) and Walter Barnhard (USGS) performed the GPR surveys that we used to locate the trench. Pat on a Cat ably navigated to and from the trench with a minimum of damage to the surrounding forest. Tom Badger and Eric Bilderback (Wash. Dept. of Transportation), Wendy Gerstel (consultant), Harvey Kelsey (Humboldt State Univ.), Karen Meyers and Michael Polenz (DGER), Alan Nelson and Ray Wells (USGS), Karl Wegmann (Lehigh Univ.), and Don West (Golder Assoc.) all provided valuable in-trench reviews and advice. Jari Roloff (DGER) prepared this poster for publication.

References Cited

Dragovich, J. D.; Logan, R. L.; Schasse, H. W.; Walsh, T. J.; Lingley, W. S., Jr.; Norman, D. K.; Gerstel, W. J.; Lapen, T. J.; Schuster, J. E.; Meyers, K. D., 2002, Geologic map of Washington—Northwest quadrant: Washington Division of Geology and Earth Resources Geologic Map GM-50, 3 sheets, scale 1:250,000, with 72 p. text.

Glassley, W. E., 1974, Geochemistry and tectonics of the Crescent volcanic rocks, Olympic Peninsula, Washington: Geological Society of America Bulletin, v. 85, no. 5, p. 785-794.

Haugerud, R. A.; Harding, D. J.; Johnson, S. Y.; Harless, J. L.; Weaver, C. S.; Sherrod, B. L., 2003, High-resolution lidar topography of the Puget Lowland, Washington—A bonanza for earth science: GSA Today, v. 13, no. 6, p. 4-10.

Johnson, S. Y.; Blakely, R. J.; Stephenson, W. J.; Dadisman, S. V.; Fisher, M. A., 2004, Active shortening of the Cascadia forearc and implications for seismic hazards of the Puget Lowland: Tectonics, v. 23, TC1011, DOI:10.1029/2003TC001507, 2004, 27 p.

Schuster, R. L.; Logan, R. L.; Pringle, P. T., 1992, Prehistoric rock avalanches in the Olympic Mountains, Washington: Science, v. 258, no. 5088, p. 1620-1621.

Sherrod, B. L.; Brocher, T. M.; Weaver, C. S.; Bucknam, R. C.; Blakely, R. J.; Kelsey, H. M.; Nelson, A. R.; Haugerud, Ralph, 2004, Holocene fault scarps near Tacoma, Washington, USA: Geology, v. 32, no. 1, p. 9-12.

Tabor, R. W.; Cady, W. M., 1978, Geologic map of the Olympic Peninsula, Washington: U.S. Geological Survey Miscellaneous Investigations Series Map I-994, 2 sheets, scale 1:125,000.

Walsh, T. J.; Korosec, M. A.; Phillips, W. M.; Logan, R. L.; Schasse, H. W., 1987, Geologic map of Washington—Southwest quadrant: Washington Division of Geology and Earth Resources Geologic Map GM-34, 2 sheets, scale 1:250,000, with 28 p. text.

Walsh, T. J.; Logan, R. L.; Neal, K. G., 1997, The Canyon River fault, an active fault in the southern Olympic Range, Washington: Washington Geology, v. 25, no. 4, p. 21-24.

Walsh, T. J.; Logan, R. L.; Neal, K. G.; Palmer, S. P., 1999, Active fault investigations on the Canyon River fault, southern Olympic Range, Washington. At U.S. Geological Survey, National Earthquake Hazards Reduction Program, External Research Program, annual project summaries, Volume 40, Pacific Northwest: U.S. Geological Survey, 20 p.

Wang, Kelin; Wells, R. E.; Mazzotti, Stephane; Hyndman, R. D.; Sagiya, Takeshi, 2003, A revised dislocation model of interseismic deformation of the Cascadia subduction zone: Journal of Geophysical Research, v. 108, no. B1, 2026, DOI:10.1029/2001JB001227, p. ETG 9-1 - 9-13.

Wells, D. L.; Coppersmith, K. J., 1994, New empirical relationships among magnitude, rupture length, rupture width, rupture area, and surface displacement: Bulletin of the Seismological Society of America, v. 84, no. 4, p. 974-1002.

Wells, R.E.; Weaver, C.S.; Blakely, R.J., 1998, Fore-arc migration in Cascadia and its neotectonic significance: Geology, v. 26, p. 759-762.

Wilson, J. R.; Bartholomew, M. J.; Carson, R. J., 1979, Late Quaternary faults and their relationship to tectonism in the Olympic Peninsula, Washington: Geology, v. 7, no. 5, p. 235-239.

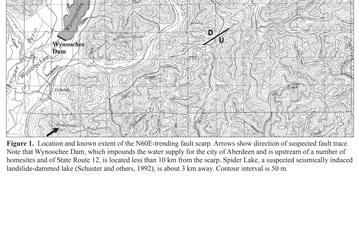

Figure 1. Location and known extent of the N60E-trending fault scarp. Arrows show direction of suspected fault trace. Note that Wynoochee Dam, which impounds the water supply for the city of Aberdeen and is upstream of a number of homesites and of State Route 12, is located less than 10 km from the scarp. Spider Lake, a suspected seismically induced landslide-dammed lake (Schuster and others, 1992), is about 3 km away. Contour interval is 50 m.

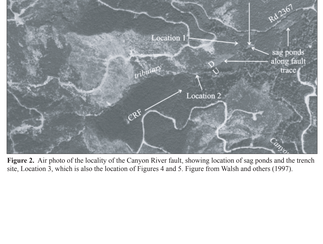

Figure 2. Air photo of the locality of the Canyon River fault, showing location of sag ponds and the trench site, Location 3, which is also the location of Figures 4 and 5. Figure from Walsh and others (1997).

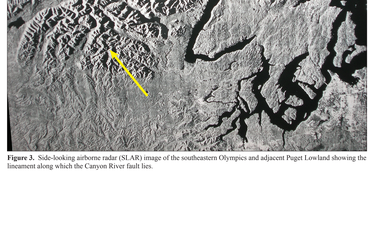

Figure 3. Side-looking airborne radar (SLAR) image of the southeastern Olympics and adjacent Puget Lowland showing the lineament along which the Canyon River fault lies.